© 2015. Published by The Company of Biologists Ltd | Development (2015) 142, 3478-3487 doi:10.1242/dev.127951

RESEARCH ARTICLE

Lin-28 promotes symmetric stem cell division and drives adaptive growth in the adult *Drosophila* intestine

Ching-Huan Chen*, Arthur Luhur* and Nicholas Sokol‡

ABSTRACT

Stem cells switch between asymmetric and symmetric division to expand in number as tissues grow during development and in response to environmental changes. The stem cell intrinsic proteins controlling this switch are largely unknown, but one candidate is the Lin-28 pluripotency factor. A conserved RNA-binding protein that is downregulated in most animals as they develop from embryos to adults, Lin-28 persists in populations of adult stem cells. Its function in these cells has not been previously characterized. Here, we report that Lin-28 is highly enriched in adult intestinal stem cells in the *Drosophila* intestine. *lin-28* null mutants are homozygous viable but display defects in this population of cells, which fail to undergo a characteristic food-triggered expansion in number and have reduced rates of symmetric division as well as reduced insulin signaling. Immunoprecipitation of Lin-28-bound mRNAs identified *Insulin-like Receptor* (*InR*), forced expression of which completely rescues *lin-28*-associated defects in intestinal stem cell number and division pattern. Furthermore, this stem cell activity of *lin-28* is independent of one well-known *lin-28* target, the microRNA let-7, which has limited expression in the intestinal epithelium. These results identify Lin-28 as a stem cell intrinsic factor that boosts insulin signaling in intestinal progenitor cells and promotes their symmetric division in response to nutrients, defining a mechanism through which Lin-28 controls the adult stem cell division patterns that underlie tissue homeostasis and regeneration.

KEY WORDS: Lin-28, Symmetric renewal, Intestinal stem cell, *Drosophila*

INTRODUCTION

The sizes of stem cell populations vary owing to changes in the ratio of symmetric versus asymmetric stem cell division, but the underlying molecular mechanisms responsible for adjusting this ratio both during tissue development and homeostasis are not clear (Morrison and Kimble, 2006; Simons and Clevers, 2011). One relevant pathway during development is the heterochronic pathway, originally identified in *Caenorhabditis elegans* for controlling the timing of cell fate specification (Rougvie and Moss, 2013). This pathway is composed of a series of factors with evolutionarily conserved temporal expression patterns. It includes the RNA-binding protein Lin-28, which is highly expressed during the early developmental stages of many animals but is downregulated as development progresses (Shyh-Chang and Daley, 2013). *lin-28* is required for symmetric divisions that expand the number of progenitor cells during the second larval stage of *C. elegans* development (Moss et al., 1997). It is thought to also promote symmetric divisions during mouse development: *Lin28a* is required for the expansion of the primordial germ cell population (Shinoda et al., 2013) and, along with its paralog *Lin28b*, expansion of the neural progenitor population during embryogenesis (Yang et al., 2015). Lin-28 expression is completely extinguished by adulthood in *C. elegans* (Moss et al., 1997), but is known to persist in vertebrate adult stem cell populations, including neuronal and spermatogonial stem cells (Cimadamore et al., 2013; Zheng et al., 2009). This post-developmental expression raises the possibility that Lin-28 adjusts adult stem cell division patterns in adult tissues as well.

Although the role of endogenous Lin-28 in these adult stem cell populations is unknown, driving Lin-28 at low levels in adult mice enhances the injury-induced repair of ear and digit tissues (Shyh-Chang et al., 2013). Such ectopic Lin-28 rejuvenates the metabolism of adult tissues, increasing insulin sensitivity, glucose metabolism and oxidative phosphorylation (Shyh-Chang et al., 2013; Zhu et al., 2011). Lin-28 also enhances the production of induced pluripotent stem cells when co-expressed with other pluripotency factors by mechanisms that remain unclear (Yu et al., 2007). Lin-28 controls gene expression in two conserved ways: by limiting the production of the microRNA let-7 and by modulating the translation of mRNAs. The *in vivo* functions of Lin-28 are at least partially independent of *let-7* (Balzer et al., 2010; Shyh-Chang et al., 2013; Vadla et al., 2012), but identifying other relevant targets of Lin-28 is a challenge because Lin-28 contacts thousands of mRNAs (Cho et al., 2012; Graf et al., 2013; Hafner et al., 2013; Madison et al., 2013; Wilbert et al., 2012).

In this study, we use *Drosophila melanogaster* to investigate the role of Lin-28 in adult stem cells. We focus on the fly intestine, an excellent model in which to study the stem cell dynamics underlying tissue homeostasis and regeneration (Lucchetta and Ohlstein, 2012). In response to nutrition, for example, the size of the intestinal stem cell (ISC) population grows (McLeod et al., 2010; O'Brien et al., 2011). Such population dynamics reflect the collective division patterns of individual ISCs, which divide in one of three ways. ISCs can divide asymmetrically to produce one ISC and one transient progenitor cell, the enteroblast (EB), which directly differentiates into either an absorptive enterocyte (EC) or a hormone-producing enteroendocrine cell (EE) (Micchelli and Perrimon, 2006; Ohlstein and Spradling, 2006). Alternatively, ISCs can undergo a symmetric differentiation division to produce two enteroblasts or a symmetric renewal division to produce two ISCs (de Navascues et al., 2012; O'Brien et al., 2011). A relative increase in symmetric renewals drives the adaptive growth of the intestine in response to nutrition, and is associated with elevated insulin signaling (O'Brien et al., 2011). Reflecting the pervasive effect of systemic insulin, Insulin-like Receptor (InR) also promotes the differentiation of enteroblasts and the size and ploidy of

Department of Biology, Indiana University, Bloomington, IN 47405, USA.
*These authors contributed equally to this work

‡Author for correspondence (nsokol@indiana.edu)

Received 29 June 2015; Accepted 20 August 2015

Development (2015) 142, 3478-3487 doi:10.1242/dev.127951

enterocytes (Choi et al., 2011). Here, we show that Lin-28 is a progenitor-cell component of the insulin/IGF signaling (IIS) pathway that boosts insulin signaling in response to nutrients and promotes the ISC symmetric renewal, driving intestinal tissue growth.

RESULTS

lin-28$^{\Delta 1}$ null homozygotes are viable

We first characterized a P-element-derived deletion that completely removes exons 2-5 of the *lin-28* locus (Fig. 1A). Because the intact first exon encoded only 33 amino acids, we considered this allele, which we named *lin-28*$^{\Delta 1}$, a putative null. Supporting this, Lin-28 protein was not detected in *lin-28*$^{\Delta 1}$ embryonic extracts (Fig. 1B). Furthermore, *lin-28*$^{\Delta 1}$ homozygotes displayed partial developmental lethality, similar to strains hemizygous for *lin-28*$^{\Delta 1}$ and a deletion that completely removed *lin-28* (Fig. 1C). Mutant animals that survived to adulthood were viable, fertile, and normally sized and featured, indicating that Lin-28 did not play an essential role in stem cells in developing animals raised under standard laboratory conditions.

Lin-28 is abundant in adult intestinal progenitor cells

Reasoning that *lin-28*$^{\Delta 1}$ adults might display defects in the homeostasis of adult tissues, we surveyed Lin-28 expression in adult stem cell populations. To do so, we prepared transgenes encoding Lin-28 fused at its C-terminus to either Venus or mCherry and under the control of *lin-28* regulatory sequences (Fig. 1A). These transgenes were functional: they restored Lin-28 protein levels as well as full viability to the *lin-28*$^{\Delta 1}$ mutant strain (Fig. 1B,C). In ovaries and testes, Lin-28::Venus was highly expressed in cap cells and hub cells, respectively, but expression was much weaker both in the germline stem cells that these

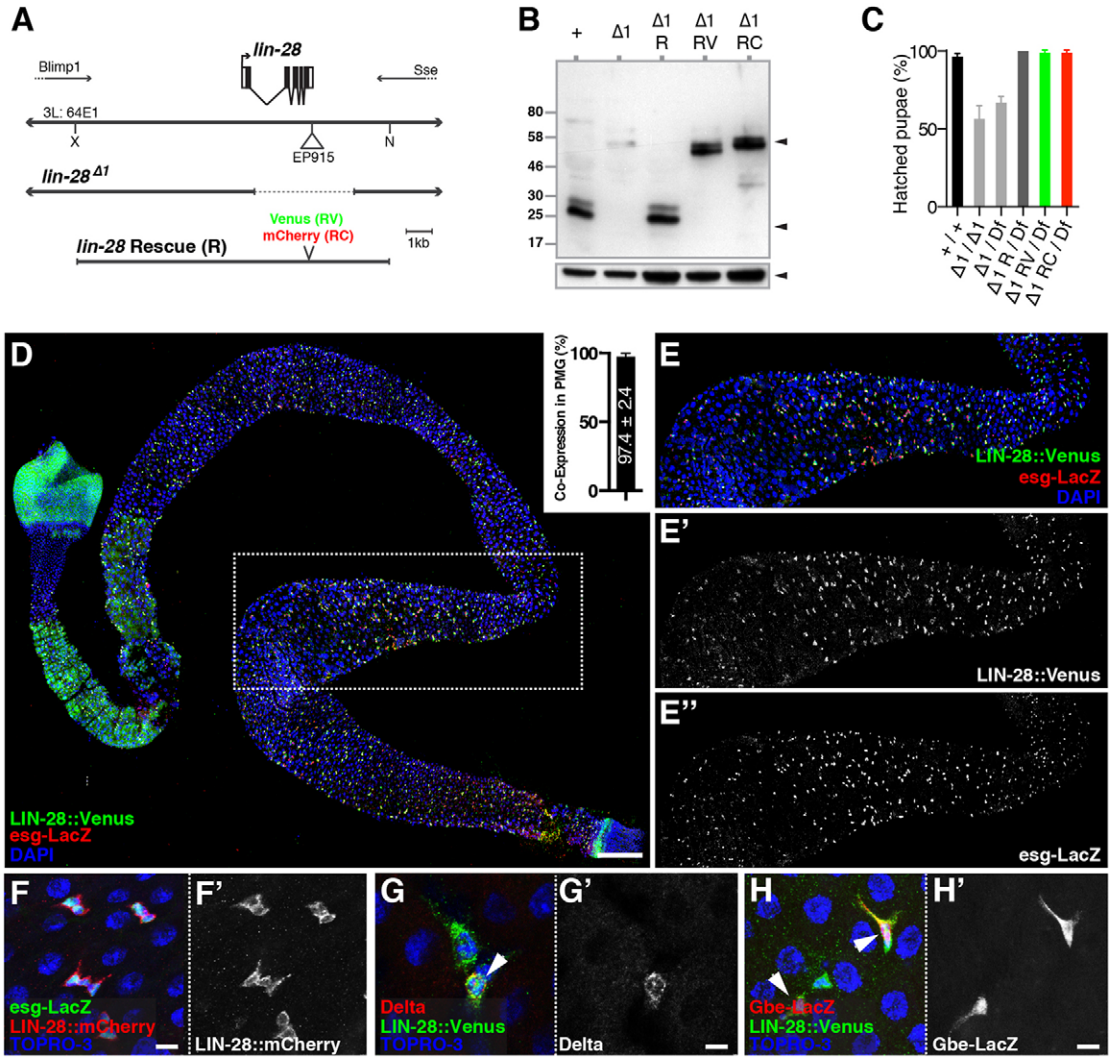

Fig. 1. Lin-28 is enriched in adult intestinal progenitor cells. (A) Schematic of the *lin-28* locus and genetic reagents, including the *lin-28* rescuing transgenes (R, RV and RC). (B) Western blot of control (+), *lin-28*$^{\Delta 1}$ (*Δ1*), *Δ1 R*, *Δ1 RV* and *Δ1 RC* embryonic extracts probed with anti-Lin-28 (top panel) or anti-Tubulin (bottom panel) antibodies. Lin-28::Venus or Lin-28::Cherry fusion proteins were detected in RV or RC extracts, respectively (top panel, top arrowhead). (C) Eclosion rates of control (+/+), *lin-28*$^{\Delta 1}$ mutant (*Δ1*/*Δ1* and *Δ1*/*Df*) and rescued *lin-28*$^{\Delta 1}$ mutant (*Δ1 R*/*Df*, *Δ1 RV*/*Df* and *Δ1 RC*/*Df*) pupae. *Df* refers to *Df(3L)Exel6106*, which removes *lin-28* and two other genes. Data are mean±s.e.m. (D) An entire intestine stained for Lin-28::Venus (anti-GFP, green), *esg-lacZ* (anti-β-gal, red) and DNA (DAPI, blue). Inset: percentage of *esg-lacZ*+ cells that are Lin-28::Venus+ (*n*=3 midguts). (E-E″) Portion of posterior midgut indicated by dotted box in D. Separate channels are shown in E′ and E″. (F) Posterior midgut epithelium stained for *esg-lacZ* (green), Lin-28::mCherry (red) and DNA (TOPRO3, blue). (G) Posterior midgut epithelium stained for Lin-28::Venus (green), Delta (red) and DNA (TOPRO3, blue). (H) Posterior midgut epithelium stained for Lin-28::Venus (green), *Su(H)-GBE-lacZ* (red) and DNA (TOPRO3, blue). F′, G′ and H′ show single channels as indicated. Scale bars: D, 100 µm; F,F′, 5 µm; G-H′, 12.5 µm.

Development (2015) 142, 3478-3487 doi:10.1242/dev.127951

niche cells physically contact as well as in nearby somatic stem cells (Fig. S1).

Although not enriched in stem cells in adult gonadal tissues, Lin-28 accumulated in almost all intestinal progenitor cells in the adult intestine (Fig. 1D-F). For example, 97.4% (n=1589) of cells positive for *escargot* (*esg*), an intestinal progenitor marker (Micchelli and Perrimon, 2006), also expressed Lin-28::Venus (Fig. 1D, inset). Consistently, Lin-28 was expressed in cells labeled by either the ISC marker Delta (Dl) (Ohlstein and Spradling, 2007) (Fig. 1G) or the enteroblast-specific marker *Su(H)-GBE-lacZ* (Micchelli and Perrimon, 2006) (Fig. 1H). By contrast, Lin-28 was much more weakly expressed in differentiated enterocytes and enteroendocrine cells (data not shown), suggesting a specific function in intestinal progenitors.

lin-28 is required for adult ISC expansion

To assess Lin-28 function in the intestinal epithelium, we conducted a census of cell types in seven-day-old control and *lin-28*$^{\Delta 1}$ mutant intestines from females raised under standard conditions (Fig. 2A-C; Fig. S2). For this experiment and others described below, we limited our analysis to the well-characterized posterior midgut (PMG) of the intestinal tract (see supplementary materials and methods for definitions of intestinal regions analyzed). Although mutant PMGs contained all known cell types, indicating that *lin-28*$^{\Delta 1}$ ISCs were multipotent (Fig. 2A-C), the total number of intestinal cells was reduced (Fig. 2C). The Delta^{+} ISC population was most affected: when normalized to the total population, *lin-28* mutant intestines contained only 73.7% of the ISCs that control intestines did (Fig. 2C′). This reduction persisted with age, but rescued *lin-28*$^{\Delta 1}$ adults displayed normal numbers of progenitor cells (Fig. 2D). Thus, the loss of Lin-28 resulted in a persistent shortage of ISCs that probably led to reduced numbers of other intestinal cell types.

To determine when *lin-28*$^{\Delta 1}$ flies first displayed this reduction, we examined ISC numbers in young adults. At eclosion, flies contain a founding population of ISCs that expand in number after feeding (O'Brien et al., 2011). Newly emerged *lin-28*$^{\Delta 1}$ mutant adults had the same number of ISCs as controls (Fig. 2E), indicating that the reduced size of the ISC population was due to an absence of expansion during adulthood rather than during development. Furthermore, although the ISC population grew 1.4-fold over a 4-day period in fed controls, ISC number shrank slightly in fed *lin-28*$^{\Delta 1}$ mutants (Fig. 2E) even though *lin-28*$^{\Delta 1}$ mutants ingested food at normal levels (Fig. S3). To analyze the ISC dynamics in response to feeding, we counted ISCs in animals fed for 3 or 18 h after a period of

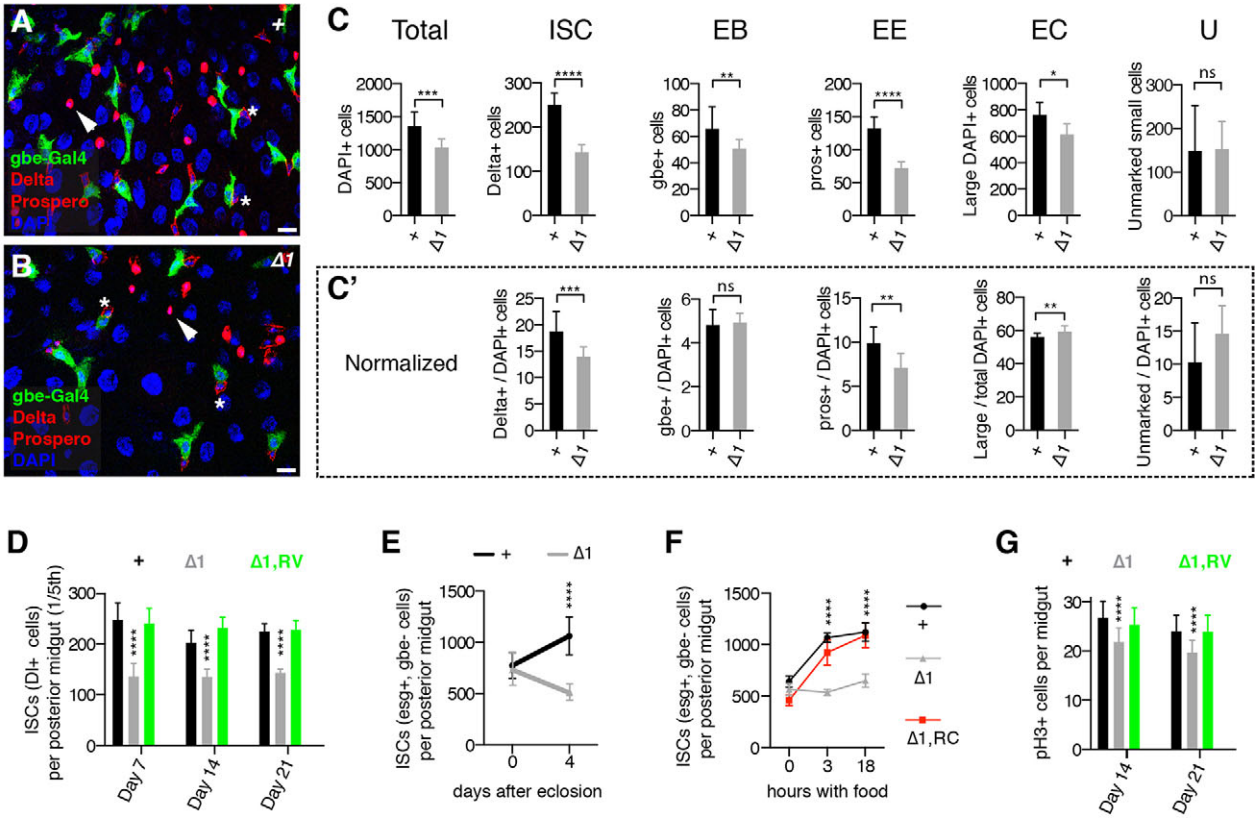

Fig. 2. Lin-28 promotes food-triggered ISC expansion. (A,B) Posterior midgut epithelia of control (A) and *lin-28*$^{\Delta 1}$ mutant (B) animals harboring *Su(H)-GBE-Gal4* and *UAS-GFP* transgenes and stained for enteroblasts (GFP, green), ISCs (Delta, cytoplasmic red), enteroendocrine cells (Prospero, nuclear red) and cell nuclei (DAPI, blue). ISCs (asterisks) and enteroendocrine cells (arrowheads) are labeled. See Fig. S2 for quantification of cell types in these images. Scale bars: 10 µm. (C) Average number of total, ISC, enteroblast (EB), enteroendocrine cell (EE), enterocyte (EC) and unmarked (U) cell types in a defined one-fifth portion of the posterior midguts of 7-day-old control (+; n=7) and *lin-28*$^{\Delta 1}$ mutant (Δ*1*; n=10) adults. (C′) Numbers of each cell type normalized to the total cell population. *P<0.05, **P<0.01, ***P<0.001, ****P<0.0001. ns, not significant. (D) Average number of Dl^{+} cells in a defined one-fifth portion of the posterior midguts of control (+), *lin-28*$^{\Delta 1}$ mutant (Δ*1*) and rescued *lin-28*$^{\Delta 1}$ mutant (Δ1,RV) adults (n=5) that were aged 7, 14 or 21 days. ****P<0.0001 for Δ*1* versus + or Δ*1*, RV. (E) Total number of ISCs (*esg*+, *Su(H)-GBE*− cells) in the entire posterior midgut of control (+) and *lin-28*$^{\Delta 1}$ mutant (Δ*1*) females at eclosion (0) or after 4 days with food. (F) Total number of ISCs (*esg*+, *Su(H)-GBE*− cells) in starved control (+), *lin-28*$^{\Delta 1}$ mutant (Δ*1*) and rescued *lin-28*$^{\Delta 1}$ mutant (Δ*1*,RC) females that were fed for 0, 3 or 18 h. (G) Average number of phospho-Histone3-positive (pH3+) cells in the intestines of control (+), *lin-28*$^{\Delta 1}$ mutant (Δ*1*) and rescued *lin-28*$^{\Delta 1}$ mutant (Δ*1*,RV) adults (n=20) aged 14 or 21 days. ****P<0.0001 for Δ*1* versus + or Δ*1*,RV. Data are mean±s.e.m.

Development (2015) 142, 3478-3487 doi:10.1242/dev.127951

starvation. ISC number and mitotic index rose sharply in controls, suggesting that ISCs in starved animals were poised to amplify in response to food (Fig. 2F; Fig. S4). By contrast, ISC number and mitotic index remained constant in *lin-28*$^{\Delta 1}$ mutants (Fig. 2F; Fig. S4). Importantly, we found no increase in the number of cells undergoing cell death in *lin-28*$^{\Delta 1}$ mutant intestines (Fig. S5), indicating that *lin-28* did not promote ISC number by repressing apoptosis; the slight reduction in ISC number in fed *lin-28*$^{\Delta 1}$ mutants (Fig. 2E) might be due to non-apoptotic cell death or perhaps cell extrusion. We also counted the total number of dividing ISCs stained for the mitotic marker phospho-Histone3 (pH3) in the midguts of animals aged 14 and 21 days to investigate whether mutant ISCs became quiescent, leading to a persistent, nonmitotic population of ISCs in aged animals. Mitotic cells were detected at these time points in *lin-28*$^{\Delta 1}$ mutant intestines (Fig. 2G), although only ~80% as many as in controls, indicating that ISCs continued to divide even in aged mutants. From these experiments, we concluded that the absence of ISC expansion displayed by *lin-28*$^{\Delta 1}$ mutants was not due to either elevated levels of cell death or the absence of ISC division.

Because loss of *lin-28* decreased ISC number, we also tested whether elevated levels of *lin-28* led to more ISCs by forcing *lin-28* expression in adult ISCs and enteroblasts for two days using the temperature-sensitive *esg*-Gal4 system (Micchelli and Perrimon, 2006). This resulted in a significant increase in the total ISC population in posterior midguts (Fig. S6A). We prepared modified transgenes containing mutations in the N-terminal cold shock domain (CSD) and C-terminal zinc finger (ZF) domains of Lin-28 to investigate whether both of these RNA-binding regions were required for this activity (Fig. S6B,C). After verifying that these mutant versions were expressed at wild-type levels (Fig. S6D-K), we found that the increase in progenitor cell numbers required the RNA-binding CSD of Lin-28 but not the ZF domains. Expression of hsLin-28A, the closest human ortholog of fly Lin-28, also increased ISC/enteroblast number (Fig. S6C,G). Thus, the activity responsible for promoting ISC number was conserved between fly and human Lin-28 and was also dosage dependent, as changes in Lin-28 levels were reflected in analogous changes in ISC population size.

lin-28 is required in adult ISC lineages to promote ISC numbers

We next employed a clonal technique, mosaic analysis with a repressible cell marker (MARCM), to induce and track single *lin-28*$^{\Delta 1}$ mutant ISC lineages in heterozygous adults. These MARCM clones were analyzed in two ways. First, intestines were scored for the total numbers of ISC-containing clones at increasing lengths of time after clone induction. This assay assesses the persistence of ISCs over time as loss of stem cell self-renewal leads to the reduction and ultimate elimination of labeled clones with age. In control intestines, clone number increased ~3.2-fold during the first two weeks of adulthood (Fig. 3A), reflecting the amplification of ISC numbers known to occur during early adult life (O'Brien et al., 2011). By contrast, the number of *lin-28*$^{\Delta 1}$ mutant clones remained constant, indicating no net gain or loss in the number of mutant ISCs. Second, we also directly counted the number of Delta^{+} ISCs per clone at 5 and 12 days after clone induction (Fig. 3B,E-G). Whereas the average number of ISCs per control clone increased from 1.2±0.4 (n=61) to 1.8±0.9 (n=94) between 5 and 12 days after clone induction, ISC number in *lin-28*$^{\Delta 1}$ mutant clones decreased slightly from 1.0±0.4 (n=53) to 0.8±0.5 (n=123) during this same time period (Fig. 3B). Taken together, both assays indicated that *lin-28* was required within adult ISC lineages to promote ISC number.

We also assessed the behavior of *lin-28*$^{\Delta 1}$ mutant ISCs by counting the total number of cells per clone (Fig. 3C,D). The average number of cells in control clones grew from 3.1±1.2 (n=61) on day 5 to 11.4±3.8 (n=94) on day 12. Cell number in *lin-28*$^{\Delta 1}$ mutant clones also grew but to a lesser extent, from 1.9±1.0 (n=53)

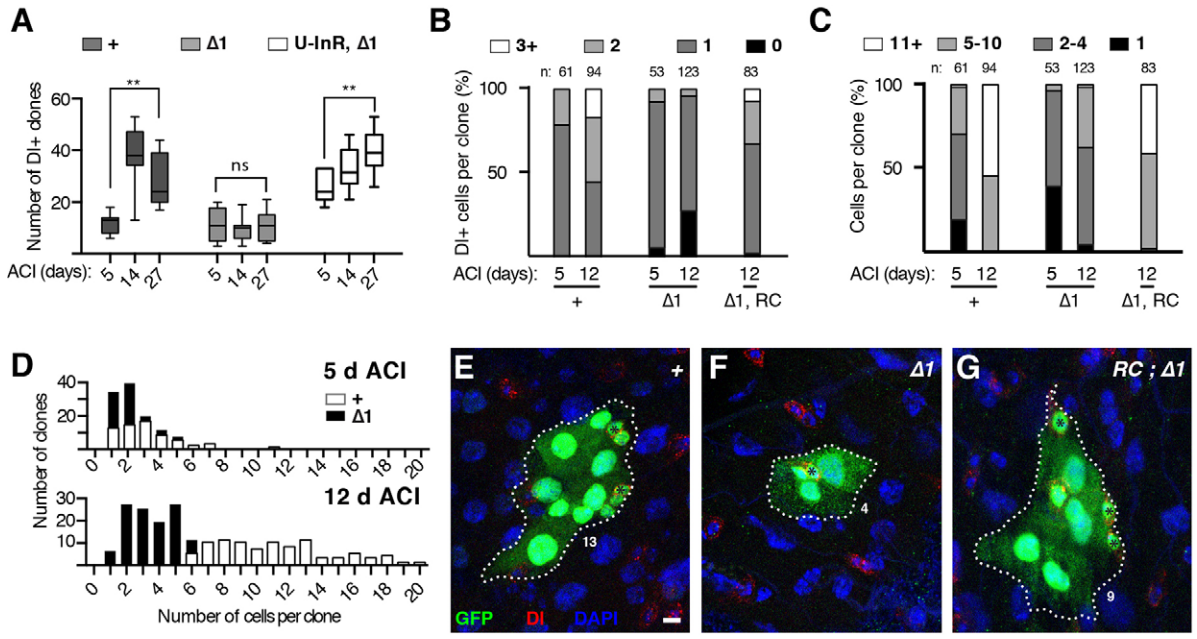

Fig. 3. *lin-28* is required in adult ISC lineages to promote ISC number. (A) Number of intestinal *tub-Gal4*, *UAS-GFP*-labeled control (+), *lin-28*$^{\Delta 1}$ (*Δ1*) and *UAS-InR*, *lin-28*$^{\Delta 1}$ (*U-InR*, *Δ1*) clones containing ISCs and present at 5, 14 and 27 days after clone induction (ACI). (B,C) Quantification of DI+ ISC (B) and total cell (C) numbers in *tub-Gal4*, *UAS-GFP*-labeled control (+), *lin-28*$^{\Delta 1}$ (*Δ1*) and rescued *lin-28*$^{\Delta 1}$ (*Δ1*, RC) clones analyzed 5 or 12 days ACI. *n*, number of clones analyzed. (D) Numbers of cells per *tub-Gal4*, *UAS-GFP*-labeled control (+) and *lin-28*$^{\Delta 1}$ (*Δ1*) clones analyzed 5 (top) and 12 (bottom) days ACI. (E-G) Representative images of *tub-Gal4*, *UAS-GFP*-labeled control (E), *lin-28*$^{\Delta 1}$ (F) and rescued *lin-28*$^{\Delta 1}$ (G) ISC clones stained for GFP (green), ISCs (Delta, red) and DAPI (blue). Clone size (dotted line), ISCs (black asterisks) and cell number are indicated. Scale bar: 5 µm.

Development (2015) 142, 3478-3487 doi:10.1242/dev.127951

on day 5 to 3.9±1.9 (n=123) on day 12 (Fig. 3D). To estimate the number of cells produced by, and by proxy the division rate of, single ISCs, we also calculated the ratio of the average number of cells in total to the average number of ISCs in all 12-day-old MARCM clones using an error propagation calculator: control clones contained 6.3 cells per ISC (range of 5.4 to 7.5, 99% confidence level, n=94) whereas *lin-28*$^{\Delta 1}$ mutant clones contained 4.7 cells per ISC (range of 4.2 to 6.2, 99% confidence level, n=123). Thus, the substantial decrease in the number of cells in *lin-28*$^{\Delta 1}$ mutant clones was due both to fewer ISCs per clone as well as a slower rate of division of individual ISCs. EdU (5-ethynyl-2′-deoxyuridine) incorporation analysis (Fig. S4G) also indicated a reduction in division rate of mutant ISCs. Taken together, these MARCM results suggested that *lin-28* accelerated ISC division rate to boost overall cell number as well as biased division pattern to amplify ISC number. This latter role was of particular interest because it was most relevant to the defect in ISC expansion.

Lin-28 promotes ISC symmetric renewal

Like any stem cell population in a cycling tissue, the size of the ISC population can vary as a result of changes in the balance between symmetric renewal, asymmetric renewal and lineage-ending symmetric differentiation (de Navascues et al., 2012; O'Brien et al., 2011) (Fig. 4A). To test directly the hypothesis that *lin-28* amplified ISC number by promoting symmetric renewal, we used a MARCM variant known as twinspot MARCM (TS-MARCM) (Yu et al., 2009). TS-MARCM marks one ISC daughter with a green label and the other with a red label so that both daughter fates can be tracked. Importantly, unlike the MARCM analysis, we induced twinspot clones in a homozygous *lin-28*$^{\Delta 1}$ mutant background rather than a heterozygous one. We scored neighboring red and green multicell clones as the product of a symmetric renewal (Fig. 4A,B), and neighboring red and green EC-like single cells with increased size as the product of symmetric differentiation (Fig. 4A,D). We relied primarily on cell number and size to characterize twinspot clones but also verified our scoring method using cell type-specific antibodies and cell ploidy analysis (see Fig. S7 and supplementary materials and methods for description of TS-MARCM characterization).

Consistent with published data (O'Brien et al., 2011), we found that the majority of ISCs (85.1%, n=215) in the PMGs of fed 2-day-old controls renewed symmetrically to produce two clusters of labeled cells (Fig. 4E). By contrast, less than half of the ISCs (40.6%, n=325) in *lin-28*$^{\Delta 1}$ mutant intestine did. This decrease in symmetric renewal was accompanied by an increase in symmetric differentiation: 17.2% of *lin-28*$^{\Delta 1}$ ISCs produced two enterocytes whereas only 0.5% of control ISCs did. These results suggest that the reduced number of ICSs in *lin-28* mutant intestines is caused by a shift in the balance of symmetric renewal versus differentiation, although we cannot rule out the possibility that mutant ISCs might also prematurely differentiate without dividing. To evaluate food uptake on ISC division patterns, we induced TS-MARCM clones in starved adults or adults that had been fed for 3 hours [Fig. 4E, (s) and (+3), respectively]. Division patterns were similar in starved controls and mutants. However, 3 hours of feeding elicited a significant ∼25% increase in symmetric renewal divisions in

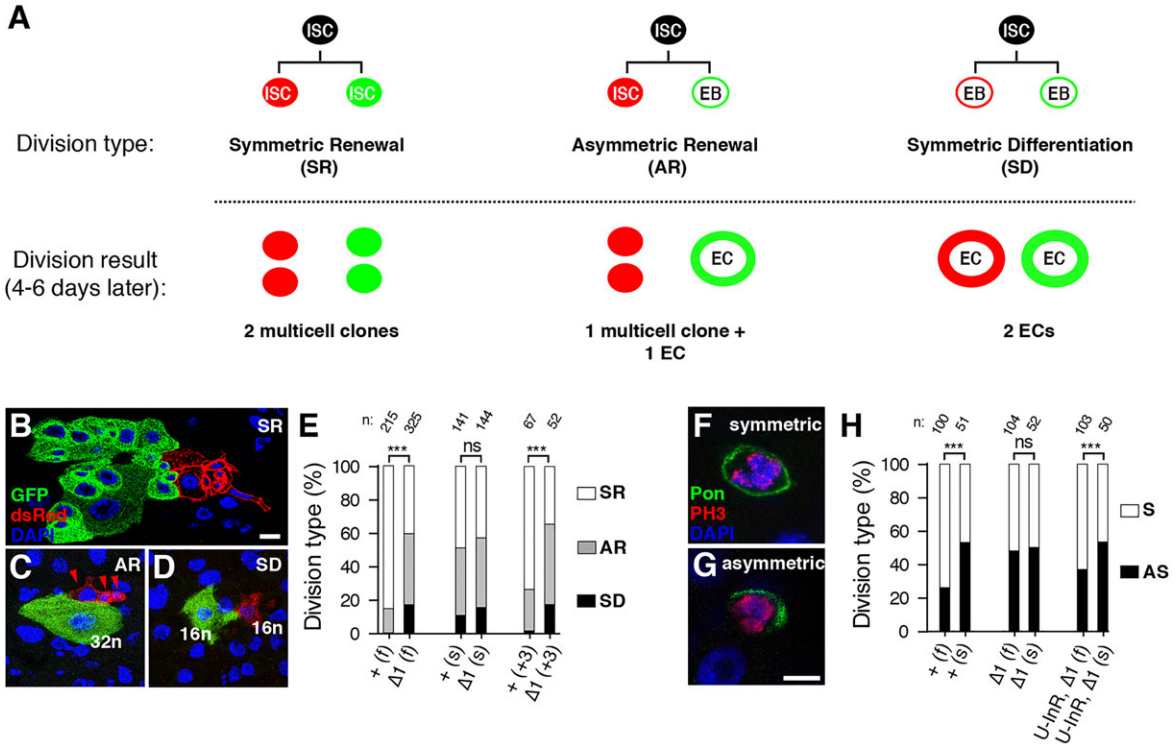

Fig. 4. Lin-28 promotes food-triggered symmetric ISC renewal. (A) Schematic of the different outcomes of three division patterns: symmetric renewal (SR), asymmetric renewal (AR) and symmetric differentiation (SD). (B-D) Representative TS-MARCM-labeled examples of the three possible division patterns. 16n, 32n; cell ploidy (see Fig. S7 on ploidy measurements). (E) Quantification of division types in fed (f), starved (s) or 3-h post-feeding (+3) control (+) and *lin-28*$^{\Delta 1}$ mutant (*Δ1*) females. (F,G) *Dl-Gal4*, *UAS-Pon::GFP*-labeled ISCs stained for GFP (green), phospho-Histone3 (red) and DNA (blue). Representative examples of symmetric (F) and asymmetric (G) divisions are shown. (H) Quantification of division types in fed (f) and starved (s) wild-type (+), *lin-28*$^{\Delta 1}$ mutant (*Δ1*) and *UAS-InR*, *lin-28*$^{\Delta 1}$ (*U-InR*, *Δ1*) females. *n*, numbers of clones analyzed; statistical significance calculated by Wald chi-square logistic regression; see Fig. S7 for statistical significance of additional pairwise comparisons. ***P<0.001. ns, not significant. Scale bars: B, 10 µm; G, 5 µm.

Development (2015) 142, 3478-3487 doi:10.1242/dev.127951

controls (P=0.008) but had no effect on ISC division patterns in mutants (P=0.313). These data indicated that *lin-28* mediated a nutrient-dependent signal within ISC lineages to control ISC division pattern.

To confirm these TS-MARCM results, we used a second method for distinguishing symmetric from asymmetric ISC divisions in homozygous control or *lin-28*$^{\Delta 1}$ mutant intestines (Kohlmaier et al., 2015). In this approach, a GFP-tagged version of the localization domain of Partner of Numb (Pon::GFP) was expressed specifically in ISCs. Symmetrically dividing ISCs displayed cortical GFP around the entire mitotic cell (Fig. 4F), whereas asymmetrically dividing ISCs displayed cortical GFP only around the basal side of the mitotic cell (Fig. 4G). Consistent with our twinspot analyses, we found no difference in the division patterns of control and *lin-28*$^{\Delta 1}$ mutant intestines in the absence of feeding (Fig. 4H). However, feeding elicited a significant increase in the percentage of symmetric divisions in controls (P=0.001) but not mutants (P=0.906). Together, the TS-MARCM and Pon::GFP analyses indicated that *lin-28* promoted symmetric renewal in response to feeding, supporting the hypothesis that reduced symmetric renewal was at least partly responsible for the absence of ISC expansion in mutant intestines.

InR signaling is reduced in *lin-28*$^{\Delta 1}$ mutant intestines

Because the IIS pathway has been implicated in the expansion of the intestinal progenitor population in response to feeding (O'Brien et al., 2011), we wondered whether insulin signaling might be altered in *lin-28*$^{\Delta 1}$ mutant intestines. We first measured the level of intestinal *insulin-like peptide 3* (*Ilp3*) transcript, which is expressed in the visceral muscle surrounding the intestine and is induced in response to food consumption (O'Brien et al., 2011). Although *Ilp3* mRNA was induced normally in *lin-28*$^{\Delta 1}$ intestines (Fig. 5A), several downstream insulin signaling components that are induced by nutrient deprivation and may poise starved cells to respond rapidly to insulin, including *Lk6* and *4e-bp* (*Thor* – FlyBase) (Puig et al., 2003; Teleman et al., 2008), were not induced in the intestines of starved *lin-28*$^{\Delta 1}$ mutants (Fig. 5B). Interestingly, we found that starvation led to an increase in *lin-28* mRNA levels along with *Lk6* and *4e-bp* in the intestines of control animals (Fig. 5B). As this result suggested a role for Lin-28 in nutrient-responsive signaling, we analyzed the membrane intensity of a tGPH pleckstrin homology domain reporter, which is known to relocate to the membrane in response to nutrients (Britton et al., 2002). Membrane-localized tGPH was abundant in the ISCs of fed animals, but much less so in fed *lin-28*$^{\Delta 1}$ mutants (compare Fig. 5C and 5D). Stem cell membrane localization of tGPH was also reduced in intestines dissected from starved *lin-28*$^{\Delta 1}$ mutants and then treated for 10 min with insulin *ex vivo* (compare Fig. 5E and 5F). Quantification of this tGPH fluorescence intensity revealed that tGPH levels in mutant ISCs were only 60.2% of control levels (control, n=84; *lin-28*$^{\Delta 1}$, n=82; P=0.0032), confirming that insulin signaling was dampened in *lin-28*$^{\Delta 1}$ mutant intestines. In addition, we analyzed the level of phosphorylated Akt (p-Akt), which is known to increase in cells receiving insulin, in intestines incubated with or without insulin (Fig. 5G,H; Fig. S8). We detected an average 9.0-fold increase in normalized p-Akt in control intestines after insulin treatment (n=3), but a significantly reduced induction of only 4.7-fold in treated *lin-28*$^{\Delta 1}$ mutant intestines (Fig. 5G,H). Because insulin signaling has also been shown to promote the size of enterocytes (Choi et al., 2011), we also measured the diameters of control and *lin-28* mutant enterocytes but found no difference between them [EC diameter in clones 12 days after clone induction (ACI): control=13.85±1.9 µm (n=50); *lin-28*$^{\Delta 1}$=13.3±2.0 µm (n=50)]. Thus, *lin-28* mutant ISCs displayed both reduced rates of symmetric renewal as well as reduced insulin signaling.

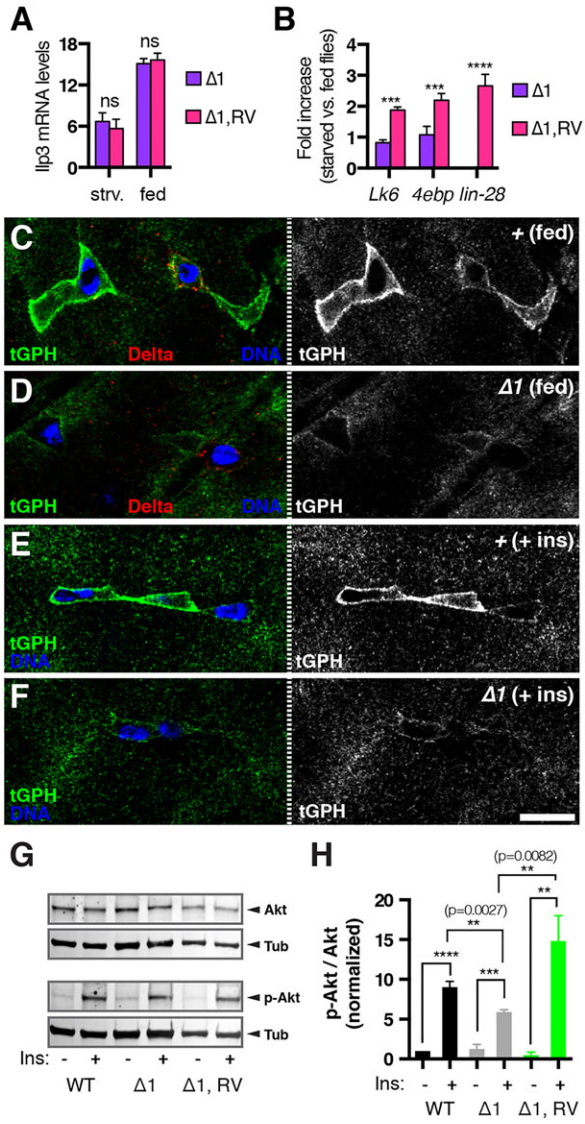

Fig. 5. Lin-28 promotes insulin signaling in intestinal progenitors. (A) *Ilp3* mRNA levels in *lin-28*$^{\Delta 1}$ (*Δ1*) and rescued *lin-28*$^{\Delta 1}$ (*Δ1*,RV) adults under starved (strv.) and fed conditions as determined by qRT-PCR. (B) Fold change in *Lk6*, *4e-bp* and *lin-28* mRNA levels in the intestines of starved versus fed *lin-28*$^{\Delta 1}$ (*Δ1*) and rescued *lin-28*$^{\Delta 1}$ (*Δ1*,RV) adults determined by qRT-PCR. ***P<0.001 for *Δ1* versus *Δ1*,RV. ns, not significant. (C,D) Fed control (C) and *lin-28*$^{\Delta 1}$ mutant (D) intestines stained for Delta (red), tGPH (green) and DNA (blue). (E,F) Insulin-treated control (E) and *lin-28*$^{\Delta 1}$ mutant (F) intestines stained for tGPH (green) and DNA (blue). Scale bar: 7.5 µm. (G) Western blot analysis of control (WT), *lin-28*$^{\Delta 1}$ mutant (*Δ1*) and rescued *lin-28*$^{\Delta 1}$ mutant (*Δ1*,RV) intestines treated with (+) or without (–) insulin and probed with anti-Akt (Akt), anti-p-Akt (p-Akt) and anti-tubulin (Tub, loading control) antibodies. (H) Quantification of average ratio of p-Akt to total Akt levels detected in three independent western blots. **P<0.01, ***P<0.001, ****P<0.0001. Data are mean±s.e.m.

Lin-28 promotes ISC number independently of the microRNA let-7

To determine the molecular basis of these defects in symmetric renewal and insulin signaling, we first evaluated whether Lin-28 promotes ISC expansion by regulating the microRNA let-7. Lin-28

Development (2015) 142, 3478-3487 doi:10.1242/dev.127951

binds to the let-7 precursor and suppresses mature let-7 production in a number of model systems (Viswanathan et al., 2008). However, this suppression only partially contributes to known Lin-28 function *in vivo* (Zhu et al., 2011; Vadla et al., 2012), indicating that Lin-28 has additional functional targets as well. In flies, loss of *lin-28* leads to elevated *let-7* levels in ovaries (Stratoulias et al., 2014) but this effect may be indirect as Lin-28 reportedly does not recognize the fly let-7 precursor (Vadla et al., 2012).

We assessed let-7 expression in *lin-28*$^{\Delta 1}$ mutant intestines using a let-7 activity sensor. After verifying this sensor in the adult nervous system where endogenous *let-7* is known to be active (Fig. S9), we compared its levels in control and *lin-28*$^{\Delta 1}$ mutant intestines. We found that intestinal GFP intensity was equivalent in these genotypes (Fig. 6A-C), indicating no inappropriate let-7 elevation in *lin-28*$^{\Delta 1}$ mutant intestines. Furthermore, consistent with recent transcriptional profiling analysis that did not detect *let-7* in purified intestinal cells from young adults (Dutta et al., 2015), three different *let-7* transcriptional reporters (Chawla and Sokol, 2012; Wu et al., 2012) were hardly detectable in the intestinal epithelium (Fig. S10). This expression analysis indicated that *let-7* was minimally expressed and probably not regulated by Lin-28 in the intestinal epithelium.

To investigate further a potential functional interaction between let-7 and Lin-28 in the intestinal epithelium, we analyzed the consequences of altered *let-7* dosage. Neither elimination nor overexpression of *let-7* in ISCs resulted in significant changes in ISC numbers (Fig. 6D,E). Furthermore, the complete elimination of *let-7* did not suppress the *lin-28*$^{\Delta 1}$ mutant defect, as might have been expected if *lin-28*$^{\Delta 1}$ mutant phenotypes were a consequence of elevated *let-7* (Fig. 6E,F). Thus, we found no evidence that Lin-28 controlled ISC expansion in young adults via a let-7-dependent mechanism.

Lin-28 physically associates with *InR* mRNA

Lin-28 can also affect mRNA translation independently of let-7 (Cho et al., 2012; Polesskaya et al., 2007; Shyh-Chang et al., 2013; Wilbert et al., 2012), raising the possibility that Lin-28 directly regulates mRNAs to promote insulin signaling and ISC symmetric renewal. To screen for such targets, we performed an RNA immunoprecipitation followed by deep sequencing (RIP-seq) experiment for Lin-28::Venus-bound mRNAs in embryos, a stage when *let-7* is not expressed. The only core IIS gene identified was *Insulin-like Receptor* (*InR*) (Table S3). Although Lin-28 is known to regulate mammalian orthologs of *InR* via let-7 (Zhu et al., 2011), the 3′UTR of fly *InR* did not contain any predicted let-7 binding sites (Lewis et al., 2005). Confirming its physical association with Lin-28, *InR* mRNA was enriched 8.9- and 3.6-fold in Lin-28 immunoprecipitates from embryos and adults, respectively (Fig. 7A; Fig. S11). This finding suggested that Lin-28 might modulate InR expression in adult intestines to promote IIS signaling and ISC symmetric renewal.

To evaluate this physical association in intestinal progenitors, we analyzed the relative subcellular expression patterns of Lin-28 protein and *InR* mRNA using a combined *in situ* hybridization/immunohistochemical approach (Toledano et al., 2012). After first verifying our InR *in situ* probes on intestinal progenitors expressing either an InR RNAi construct or an InR cDNA (Fig. 7B,C), we compared the expression patterns of Lin-28::Venus with *InR* mRNA in intestinal progenitors (Fig. 7D). Lin-28::Venus was detected in numerous cytoplasmic punctae, and *InR* mRNA was detected in some of these as well (Fig. 7D, arrowhead). Thus, although Lin-28::Venus and *InR* mRNA did not exhibit identical expression patterns in intestinal progenitors, this result suggested that the physical association between Lin-28 and *InR* also occurred in adult intestinal progenitors.

Restoration of InR signaling rescues *lin-28*$^{\Delta 1}$ mutant ISC numbers

To investigate whether Lin-28 might promote IIS signaling via InR, we examined whether elevation of Lin-28 in intestinal progenitors enhanced InR levels. Because intestinal InR levels were below the level of detection, we also induced *InR* transcription by co-expressing the *InR* transcriptional activator FoxO (Puig et al., 2003). Without elevated Lin-28, InR protein was not detected in intestinal epithelia containing *esg*-Gal4-driven FoxO (Fig. 7E, arrowheads). However, InR was clearly detected in intestinal cells when both FoxO and Lin-28 were driven (Fig. 7F, arrowheads), indicating that Lin-28 promoted InR expression in this sensitized background.

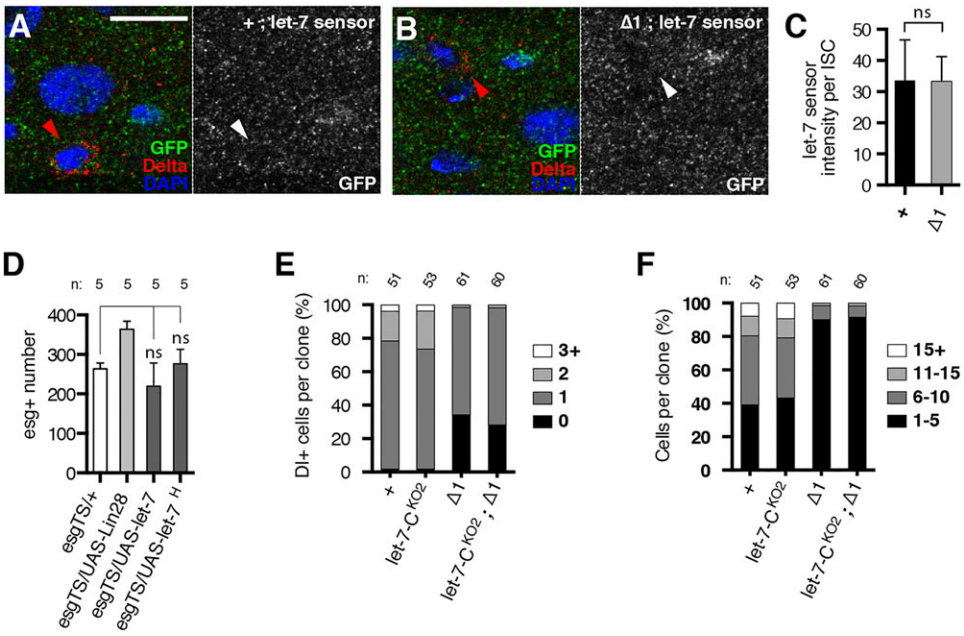

Fig. 6. *lin-28* phenotypes are not due to altered let-7 activity in ISCs. (A,B) Sections of control (A) and *lin-28*$^{\Delta 1}$ mutant (B) intestinal epithelium harboring a let-7 sensor and stained for the sensor (GFP, green), ISCs (Delta, red) and DNA (DAPI, blue). Arrowheads point to Dl^{+} ISCs. Scale bar: 10 µm. (C) let-7 sensor fluorescence intensity in control (+; *n*=100) and *lin-28*$^{\Delta 1}$ mutant (*Δ1*; *n*=134) ISCs. (D) Average number of *esg*$^{+}$ cells in a portion of the posterior midgut in *esgTS*/+, *esgTS*/*UAS-Lin-28*, *esgTS*/*UAS-let-7* and *esgTS*/*UAS-let-7*^{H} flies. (E,F) Quantification of Dl+ ISC (E) and total cell (F) numbers in controls, *let-7-C*^{KO2}, *lin-28*$^{\Delta 1}$ mutants and *let-7-C*^{KO2}; *lin-28*$^{\Delta 1}$ double mutants analyzed 10 days ACI. *n*, number of clones analyzed. Data are mean±s.e.m. ns, not significant.

Development (2015) 142, 3478-3487 doi:10.1242/dev.127951

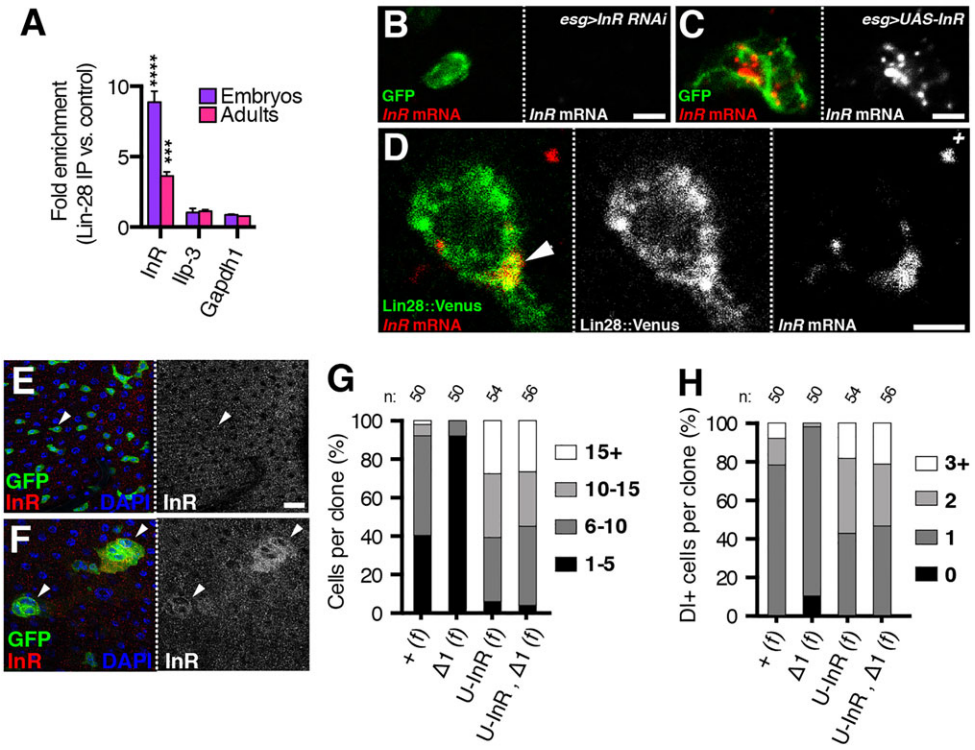

Fig. 7. Lin-28 physically associates with *InR* mRNA and InR rescues food-triggered increase of *lin-28*$^{\Delta 1}$ ISCs. (A) Fold enrichment of *InR*, *Ilp3* and *Gapdh1* mRNAs in Lin-28 versus control immunoprecipitates from embryos and adults detected by qRT-PCR. ****P<0.0001 and ***P<0.001 for enrichment of *InR* versus *Ilp-3* or *Gapdh1* in embryos or adults, respectively. Data are mean±s.e.m. (B,C) Intestinal progenitors from flies harboring *esgGal4, UAS-GFP* and either *UAS-InR*^{RNAi} (B) or *UAS-InR* (C) stained for GFP (green) and *InR* mRNA (red). (D) Colocalization of Lin-28::Venus (green) and *InR* mRNA (red) in intestinal progenitors. (E,F) Representative sections of the posterior midguts of females carrying *esg-gal4*, *UAS-GFP*, *UAS-FoxO*, *tubGal80*^{ts} alone (E) or with *UAS-Lin-28::FLAG-HA* (F) and stained for GFP (green), InR (red) and DNA (blue). (G,H) Quantification of total cell number (G) and Dl+ ISC number (H) in *tub-Gal4*, *UAS-GFP*-labeled control (+), *lin-28*$^{\Delta 1}$ (*Δ1*) and UAS-InR (U-InR or U-InR, *Δ1*) clones generated in fed (f) females and analyzed 10 days ACI. *n*, number of clones analyzed. Scale bars: B,C, 2.5 µm; D, 5 µm; E, 20 µm.

This result provided support for the hypothesis that the elevated expression of Lin-28 in intestinal progenitors led to elevated InR levels, which, in turn, promoted symmetric renewal after food intake.

If reduced InR expression caused the *lin-28*$^{\Delta 1}$-associated reduction in both ISC number and symmetric renewal, then restoration of InR levels should rescue both of these phenotypes. To test this hypothesis, we used the MARCM technique to express a *UAS-InR* transgene encoding the wild-type InR protein in *lin-28*$^{\Delta 1}$ mutant ISC clones. After verifying that these UAS-InR clones contained elevated InR levels (Fig. S12A-D), we found that both total cell numbers as well as ISC numbers were rescued in *lin-28*$^{\Delta 1}$ mutant clones present in fed animals (Fig. 7G,H). For example, only 2% of *lin-28*$^{\Delta 1}$ mutant clones contained two or more Dl^{+} ISCs at 10 days, whereas 53% of *lin-28*$^{\Delta 1}$ mutant lineages expressing InR contained two or more Dl^{+} ISCs at the same time point (Fig. 7H). Importantly, unlike constitutively active InR, this InR transgene did not restore ISC numbers to *lin-28*$^{\Delta 1}$ lineages present in starved animals (Fig. S12E-F), indicating that its forced expression did not lead to ligand-independent activation. In addition, forced expression of components of the Yorkie, Epidermal Growth Factor Receptor, and Wingless pathways did not rescue *lin-28*$^{\Delta 1}$ mutant clones (Fig. S13) even though these factors are known to increase ISC numbers (Karpowicz et al., 2010; Lee et al., 2009; Lin et al., 2008; Ren et al., 2010). Thus, these results indicated that the rescue by InR was at least somewhat specific and suggested that the failure of ISCs to expand in *lin-28*$^{\Delta 1}$ mutants was due to reduced ligand-dependent activation of InR.

Finally, confirming that InR also restored symmetric renewal to *lin-28*$^{\Delta 1}$ mutant ISCs, we found that UAS-InR led to an increase in the number of *lin-28*$^{\Delta 1}$ mutant clones per intestine over time (Fig. 3A), indicating an increase in ISC number consistent with increased symmetric renewal. In addition, UAS-InR also restored the food-triggered increase in symmetric division to *lin-28*$^{\Delta 1}$ mutant ISCs (Fig. 4H). Taken together, these results indicated that the reduced symmetric renewal displayed by *lin-28*$^{\Delta 1}$ mutant ISCs was due to reduced InR levels.

DISCUSSION

Here, we report that the RNA-binding protein Lin-28 enhances insulin signaling in ISCs and promotes their symmetric renewal independently of *let-7*. This conclusion is based on observations that Lin-28 is enriched in intestinal progenitor cells; that the founding population of ISCs fail to expand in adult *lin-28* mutants; that *lin-28* mutant ISCs display reduced rates of symmetric renewal as well as reduced insulin signaling; that Lin-28 physically associates with *InR* mRNA; and that forced expression of InR rescues *lin-28*-associated defects in ISC number and symmetric division rates. Building on these results, we propose a model in which Lin-28 boosts InR levels specifically in progenitor cells during nutrient deprivation. Elevated InR sensitizes ISCs to insulin, poising them to divide symmetrically and thereby driving the expansion of the intestinal epithelium that will maximize nutrient absorption after feeding. More generally, our findings suggest that stem cell competition for insulin, based on cell intrinsic levels of InR, might contribute to the stem cell population dynamics that underlie tissue growth and homeostasis of cycling tissues (Simons and Clevers, 2011).

Although Lin-28 modulates insulin signaling specifically within progenitor cells, it is not a constitutive component of the IIS pathway. Unlike null alleles in core *InR* pathway components (Brogiolo et al., 2001), *lin-28* mutants are viable, proceed through development on schedule, and are of normal size. In addition, *lin-28* is dispensable in the intestine for some events known to require *InR*, such as growth of enterocytes (Choi et al., 2011). Furthermore, even in progenitor cells, *lin-28* null mutant phenotypes are weaker than those previously described for *InR* null alleles: *InR* is required for cell division (Amcheslavsky et al., 2009; Biteau et al., 2010; Choi et al., 2011; O'Brien et al., 2011), whereas *lin-28* is required for food-triggered elevations in proliferation and symmetric renewal

Development (2015) 142, 3478-3487 doi:10.1242/dev.127951

rates. These observations indicate that some basal level of insulin signaling occurs in the absence of Lin-28 and that Lin-28 boosts insulin signaling in certain cells under certain conditions.

An open question relevant to our model is precisely how Lin-28 affects division pattern. Most simply, enhanced insulin signaling during cell division might promote stem cell identity by increasing the metabolism and/or size of both daughters. However, we cannot rule out the possibility that Lin-28 might affect cell polarity via, for example, the Par complex (Goulas et al., 2012), although we have not detected asymmetric localization of Lin-28 during ISC division. Furthermore, Lin-28 activity could also repress Notch signaling, as lower Notch activity leads to ISC expansion (de Navascues et al., 2012). However, such an effect is likely to be indirect because no components of the Notch pathway were found in the Lin-28 immunoprecipitation (Table S3).

Although Lin-28 has been implicated in translational control in vertebrate systems (Polesskaya et al., 2007), the precise mechanism remains unknown. The work presented here suggests that Lin-28 might directly regulate the translation of the *InR* mRNA, perhaps via its 5′UTR. Translation of *InR* mRNA is known to be post-transcriptionally stimulated via its 5′UTR in a cap-independent manner (Marr et al., 2007). This probably leads to elevated levels of InR protein in nutrient-deprived cells, which sensitizes them to insulin and thereby ensures a rapid response when growth conditions are restored. Lin-28 might also regulate InR via a 3′UTR mechanism, as it was recently shown that the microRNA miR-305 negatively regulates InR levels in ISCs via its 3′UTR (Foronda et al., 2014).

During *C. elegans* development, LIN-28 promotes symmetric division of progenitor cells independently of *let-7* and related microRNAs (Moss et al., 1997; Vadla et al., 2012). Thus, the well-characterized negative feedback between Lin-28 and *let-7* might, in general, be ancillary to their main functions *in vivo*. Future work will determine whether endogenous Lin-28 promotes the expansion of vertebrate stem cell populations, such as primordial germ cells and neuronal stem cells (Shinoda et al., 2013; Yang et al., 2015), by boosting the proportion of stem cells undergoing symmetric renewal.

MATERIALS AND METHODS

Drosophila strains and husbandry

See Table S1 for a complete list of all genotypes used in each figure. The *lin-28*$^{\Delta 1}$ mutant was obtained from a P-element excision screen of the EP915 insertion that was performed in the laboratory of Ward Odenwald (NIH). This strain harbors a 3687 bp deletion that removes all *lin-28* exons except for the first one. *w*^{1118} was used as the control strain. New transgenics were generated by Rainbow Transgenic Flies, (CA, USA). Details regarding transgene construction can be found in the supplementary materials and methods. Stocks with multiple genetic elements were obtained by meiotic recombination and/or genetic crosses.

Experimental strains were cultured on standard cornmeal media at 18°C, 25°C and 29°C in incubators set for a 12-h light/dark schedule. Starved flies were maintained in empty vials containing a tissue wetted with 1% sucrose/water solution that was refreshed daily. For *esgTS* experiments, flies were grown at 18°C until eclosion. They were then collected over 1-2 days, shifted to 29°C for 2 days, and dissected. MARCM crosses were grown at 25°C whereas twinspot MARCM crosses were grown at 18°C until heat shock and then at 25°C thereafter. Adult females were analyzed for all experiments unless otherwise indicated.

Antibody generation and western blot analysis

Antibodies were generated in rats (Cocalico Biologicals) against a His-tagged version of full-length Lin-28-PA protein that was expressed and purified according to standard methods (Cultivation and Bioprocessing Facility, Indiana University). See supplementary materials and methods for details on western blot analysis.

Dissection, immunostaining and microscopy

Adult females were dissected in 1× PBS. Gastrointestinal tracts were fixed at room temperature for either 45-60 min in 4% paraformaldehyde (Electron Microscopy Services) in PBS or 15 min in a 1:1 mixture of 4% paraformaldehyde/PBS and heptane. These samples were washed with 100% methanol and were gradually rehydrated via a 1× PBT (1× PBS, 0.3% Triton X-100)/methanol series. All samples were then blocked (1× PBT, 0.5% bovine serum albumin) for at least 1 h and then incubated at 4°C overnight with primary antibodies, including rabbit anti-β-gal (08559761, MP Biomedicals; 1:1000), mouse anti-β-gal (Z3781, Promega; 1:1000), rabbit anti-GFP (A11122, Life Technologies; 1:1000), chicken anti-GFP (600-901-215, Rockland Immunochemicals; 1:1000), rabbit anti-mCherry (5993-100, BioVision; 1:1000), rabbit anti-dsRed (632496, Clontech; 1:1000), mouse anti-Delta [C594.9b-c, Developmental Studies Hybridoma Bank (DSHB); 1:1000], mouse anti-Prospero (MR1A-c, DHSB; 1:1000), mouse anti-Armadillo (N2 7A1, DSHB; 1:100), mouse anti-GFP (DSHB-GFP-12E6, DSHB; 1:200), rabbit anti-phospho-Histone3 (9701s, Cell Signaling; 1:1000), rabbit-anti-Pdm1 (Xiaohang Yang and Yu Cai, Temasek Life Sciences Laboratory, Singapore; 1:1000) and rabbit anti-dINR (Michael Marr, Brandeis University, Waltham, MA, USA; 1:200). Samples were washed and incubated for three hours with secondary antibodies, including AlexaFluor-488 and -568-conjugated goat anti-rabbit, -chicken, -mouse and -rat antibodies (Life Technologies; 1:1000). Samples were washed again, treated with DAPI (1:10,000) or TOPRO3 (Life Technologies, 1:1000) and mounted in Vectashield mounting medium (Vector Laboratories). Images were collected on a Leica SP5 confocal microscope (Light Microscopy Imaging Center, Indiana University). The same methods were used for anti-phospho-Akt (4054s, Cell Signaling; 1:200) staining, except that TBS was used in the dissection, fixative and staining solutions. For insulin stimulation, intestines from animals starved for 4 days were incubated in M3+BPYE media supplemented with human insulin (Sigma I-9278; 1:750) for 10 min prior to fixation. For co-detection of *InR* mRNA and Lin-28::Venus protein, a published protocol (Toledano et al., 2012) was followed using six nonoverlapping digoxygenin-labeled antisense *InR* RNA probes. See supplementary materials and methods for details on MARCM and TS-MARCM clone induction and analysis, census analysis, EdU incorporation analysis, and fluorescence quantification.

Statistical analysis

All *P* values were calculated using a two-tailed unpaired *t*-test (Graphpad Prism) except for the *P* values in Fig. 4 and Fig. S6, which were calculated using a Wald χ^2 logistic regression analysis (SPSS). Average values are presented as mean±s.e.m. Unless otherwise noted, **P*<0.05, ***P*<0.01, ****P*<0.001 and *****P*<0.0001.

RNA isolation, qPCR, RIP-qPCR and RIP-seq

Total RNA was isolated using Trizol (Invitrogen). RNA destined for qPCR analysis was treated with DNAse (NEB) for 1 h at 37°C prior to phenol chloroform extraction. cDNA was synthesized using Superscript III (Invitrogen) and gene-specific reverse primers. See supplementary materials and methods for list of qPCR oligos (Table S2) as well as a more detailed description of RNA methods.

Acknowledgements

We thank Konrad Basler, Elizabeth Gavis, Ken Irvine, Michael Marr, Craig Micchelli, Eric Moss, Ward Odenwald, Norbert Perrimon, Barret Pfeiffer, Xiankun Zeng, BACPAC resources, the Bloomington and Kyoto *Drosophila* Stock Centers, and the Developmental Studies Hybridoma Bank for reagents; Doug Rusch for informatics support; and Wesley Beaulieu and Devon Hardman for statistics support.

Competing interests

The authors declare no competing or financial interests.

Author contributions

C.-H.C., A.L. and N.S. designed, performed and interpreted experiments; N.S. wrote the manuscript and C.-H.C. and A.L. edited it.

Development (2015) 142, 3478-3487 doi:10.1242/dev.127951

Funding
This work was funded by the National Institutes of Health [R01MH087511 and R21OD019916]. Deposited in PMC for release after 12 months.

Supplementary information
Supplementary information available online at
http://dev.biologists.org/lookup/suppl/doi:10.1242/dev.127951/-/DC1

References

Amcheslavsky, A., Jiang, J. and Ip, Y. T. (2009). Tissue damage-induced intestinal stem cell division in Drosophila. *Cell Stem Cell* **4**, 49-61.
Balzer, E., Heine, C., Jiang, Q., Lee, V. M. and Moss, E. G. (2010). LIN28 alters cell fate succession and acts independently of the let-7 microRNA during neurogliogenesis in vitro. *Development* **137**, 891-900.
Biteau, B., Karpac, J., Supoyo, S., Degennaro, M., Lehmann, R. and Jasper, H. (2010). Lifespan extension by preserving proliferative homeostasis in Drosophila. *PLoS Genet.* **6**, e1001159.
Britton, J. S., Lockwood, W. K., Li, L., Cohen, S. M. and Edgar, B. A. (2002). Drosophila's insulin/PI3-kinase pathway coordinates cellular metabolism with nutritional conditions. *Dev. Cell* **2**, 239-249.
Brogiolo, W., Stocker, H., Ikeya, T., Rintelen, F., Fernandez, R. and Hafen, E. (2001). An evolutionarily conserved function of the Drosophila insulin receptor and insulin-like peptides in growth control. *Curr. Biol.* **11**, 213-221.
Chawla, G. and Sokol, N. S. (2012). Hormonal activation of let-7-C microRNAs via EcR is required for adult Drosophila melanogaster morphology and function. *Development* **139**, 1788-1797.
Cho, J., Chang, H., Kwon, S. C., Kim, B., Kim, Y., Choe, J., Ha, M., Kim, Y. K. and Kim, V. N. (2012). LIN28A is a suppressor of ER-associated translation in embryonic stem cells. *Cell* **151**, 765-777.
Choi, N. H., Lucchetta, E. and Ohlstein, B. (2011). Nonautonomous regulation of Drosophila midgut stem cell proliferation by the insulin-signaling pathway. *Proc. Natl. Acad. Sci. USA* **108**, 18702-18707.
Cimadamore, F., Amador-Arjona, A., Chen, C., Huang, C.-T. and Terskikh, A. V. (2013). SOX2-LIN28/let-7 pathway regulates proliferation and neurogenesis in neural precursors. *Proc. Natl. Acad. Sci. USA* **110**, E3017-E3026.
de Navascues, J., Perdigoto, C. N., Bian, Y., Schneider, M. H., Bardin, A. J., Martinez-Arias, A. and Simons, B. D. (2012). Drosophila midgut homeostasis involves neutral competition between symmetrically dividing intestinal stem cells. *EMBO J.* **31**, 2473-2485.
Dutta, D., Dobson, A. J., Houtz, P. L., Glasser, C., Revah, J., Korzelius, J., Patel, P. H., Edgar, B. A. and Buchon, N. (2015). Regional cell-specific transcriptome mapping reveals regulatory complexity in the adult Drosophila midgut. *Cell Rep.* **12**, 346-358.
Foronda, D., Weng, R., Verma, P., Chen, Y.-W. and Cohen, S. M. (2014). Coordination of insulin and Notch pathway activities by microRNA miR-305 mediates adaptive homeostasis in the intestinal stem cells of the Drosophila gut. *Genes Dev.* **28**, 2421-2431.
Goulas, S., Conder, R. and Knoblich, J. A. (2012). The Par complex and integrins direct asymmetric cell division in adult intestinal stem cells. *Cell Stem Cell* **11**, 529-540.
Graf, R., Munschauer, M., Mastrobuoni, G., Mayr, F., Heinemann, U., Kempa, S., Rajewsky, N. and Landthaler, M. (2013). Identification of LIN28B-bound mRNAs reveals features of target recognition and regulation. *RNA Biol.* **10**, 1146-1159.
Hafner, M., Max, K. E. A., Bandaru, P., Morozov, P., Gerstberger, S., Brown, M., Molina, H. and Tuschl, T. (2013). Identification of mRNAs bound and regulated by human LIN28 proteins and molecular requirements for RNA recognition. *RNA* **19**, 613-626.
Karpowicz, P., Perez, J. and Perrimon, N. (2010). The Hippo tumor suppressor pathway regulates intestinal stem cell regeneration. *Development* **137**, 4135-4145.
Kohlmaier, A., Fassnacht, C., Jin, Y., Reuter, H., Begum, J., Dutta, D. and Edgar, B. A. (2015). Src kinase function controls progenitor cell pools during regeneration and tumor onset in the Drosophila intestine. *Oncogene* **34**, 2371-2384.
Lee, W.-C., Beebe, K., Sudmeier, L. and Micchelli, C. A. (2009). Adenomatous polyposis coli regulates Drosophila intestinal stem cell proliferation. *Development* **136**, 2255-2264.
Lewis, B. P., Burge, C. B. and Bartel, D. P. (2005). Conserved seed pairing, often flanked by adenosines, indicates that thousands of human genes are microRNA targets. *Cell* **120**, 15-20.
Lin, G., Xu, N. and Xi, R. (2008). Paracrine Wingless signalling controls self-renewal of Drosophila intestinal stem cells. *Nature* **455**, 1119-1123.
Lucchetta, E. M. and Ohlstein, B. (2012). The Drosophila midgut: a model for stem cell driven tissue regeneration. *Wiley Interdiscip. Rev. Dev. Biol.* **1**, 781-788.
Madison, B. B., Liu, Q., Zhong, X., Hahn, C. M., Lin, N., Emmett, M. J., Stanger, B. Z., Lee, J.-S. and Rustgi, A. K. (2013). LIN28B promotes growth and tumorigenesis of the intestinal epithelium via Let-7. *Genes Dev.* **27**, 2233-2245.
Marr, M. T., II, D'Alessio, J. A., Puig, O. and Tjian, R. (2007). IRES-mediated functional coupling of transcription and translation amplifies insulin receptor feedback. *Genes Dev.* **21**, 175-183.
McLeod, C. J., Wang, L., Wong, C. and Jones, D. L. (2010). Stem cell dynamics in response to nutrient availability. *Curr. Biol.* **20**, 2100-2105.
Micchelli, C. A. and Perrimon, N. (2006). Evidence that stem cells reside in the adult Drosophila midgut epithelium. *Nature* **439**, 475-479.
Morrison, S. J. and Kimble, J. (2006). Asymmetric and symmetric stem-cell divisions in development and cancer. *Nature* **441**, 1068-1074.
Moss, E. G., Lee, R. C. and Ambros, V. (1997). The cold shock domain protein LIN-28 controls developmental timing in C. elegans and is regulated by the lin-4 RNA. *Cell* **88**, 637-646.
O'Brien, L. E., Soliman, S. S., Li, X. and Bilder, D. (2011). Altered modes of stem cell division drive adaptive intestinal growth. *Cell* **147**, 603-614.
Ohlstein, B. and Spradling, A. (2006). The adult Drosophila posterior midgut is maintained by pluripotent stem cells. *Nature* **439**, 470-474.
Ohlstein, B. and Spradling, A. (2007). Multipotent Drosophila intestinal stem cells specify daughter cell fates by differential notch signaling. *Science* **315**, 988-992.
Polesskaya, A., Cuvellier, S., Naguibneva, I., Duquet, A., Moss, E. G. and Harel-Bellan, A. (2007). Lin-28 binds IGF-2 mRNA and participates in skeletal myogenesis by increasing translation efficiency. *Genes Dev.* **21**, 1125-1138.
Puig, O., Marr, M. T., Ruhf, M. L. and Tjian, R. (2003). Control of cell number by Drosophila FOXO: downstream and feedback regulation of the insulin receptor pathway. *Genes Dev.* **17**, 2006-2020.
Ren, F., Wang, B., Yue, T., Yun, E.-Y., Ip, Y. T. and Jiang, J. (2010). Hippo signaling regulates Drosophila intestine stem cell proliferation through multiple pathways. *Proc. Natl. Acad. Sci. USA* **107**, 21064-21069.
Rougvie, A. E. and Moss, E. G. (2013). Developmental transitions in *C. elegans* larval stages. *Curr. Top. Dev. Biol.* **105**, 153-180.
Shinoda, G., De Soysa, T. Y., Seligson, M. T., Yabuuchi, A., Fujiwara, Y., Huang, P. Y., Hagan, J. P., Gregory, R. I., Moss, E. G. and Daley, G. Q. (2013). Lin28a regulates germ cell pool size and fertility. *Stem Cells* **31**, 1001-1009.
Shyh-Chang, N. and Daley, G. Q. (2013). Lin28: primal regulator of growth and metabolism in stem cells. *Cell Stem Cell* **12**, 395-406.
Shyh-Chang, N., Zhu, H., Yvanka de Soysa, T., Shinoda, G., Seligson, M. T., Tsanov, K. M., Nguyen, L., Asara, J. M., Cantley, L. C. and Daley, G. Q. (2013). Lin28 enhances tissue repair by reprogramming cellular metabolism. *Cell* **155**, 778-792.
Simons, B. D. and Clevers, H. (2011). Strategies for homeostatic stem cell self-renewal in adult tissues. *Cell* **145**, 851-862.
Stratoulias, V., Heino, T. I. and Michon, F. (2014). Lin-28 regulates oogenesis and muscle formation in Drosophila melanogaster. *PLoS ONE* **9**, e101141.
Teleman, A. A., Hietakangas, V., Sayadian, A. C. and Cohen, S. M. (2008). Nutritional control of protein biosynthetic capacity by insulin via Myc in Drosophila. *Cell Metab.* **7**, 21-32.
Toledano, H., D'Alterio, C., Loza-Coll, M. and Jones, D. L. (2012). Dual fluorescence detection of protein and RNA in Drosophila tissues. *Nat. Protoc.* **7**, 1808-1817.
Vadla, B., Kemper, K., Alaimo, J., Heine, C. and Moss, E. G. (2012). lin-28 controls the succession of cell fate choices via two distinct activities. *PLoS Genet.* **8**, e1002588.
Viswanathan, S. R., Daley, G. Q. and Gregory, R. I. (2008). Selective blockade of microRNA processing by Lin28. *Science* **320**, 97-100.
Wilbert, M. L., Huelga, S. C., Kapeli, K., Stark, T. J., Liang, T. Y., Chen, S. X., Yan, B. Y., Nathanson, J. L., Hutt, K. R., Lovci, M. T. et al. (2012). LIN28 binds messenger RNAs at GGAGA motifs and regulates splicing factor abundance. *Mol. Cell* **48**, 195-206.
Wu, Y.-C., Chen, C.-H., Mercer, A. and Sokol, N. S. (2012). Let-7-complex microRNAs regulate the temporal identity of Drosophila mushroom body neurons via chinmo. *Dev. Cell* **23**, 202-209.
Yang, M., Yang, S.-L., Herrlinger, S., Liang, C., Dzieciatkowska, M., Hansen, K. C., Desai, R., Nagy, A., Niswander, L., Moss, E. G. et al. (2015). Lin28 promotes the proliferative capacity of neural progenitor cells in brain development. *Development* **142**, 1616-1627.
Yu, J., Vodyanik, M. A., Smuga-Otto, K., Antosiewicz-Bourget, J., Frane, J. L., Tian, S., Nie, J., Jonsdottir, G. A., Ruotti, V., Stewart, R. et al. (2007). Induced pluripotent stem cell lines derived from human somatic cells. *Science* **318**, 1917-1920.
Yu, H.-H., Chen, C.-H., Shi, L., Huang, Y. and Lee, T. (2009). Twin-spot MARCM to reveal the developmental origin and identity of neurons. *Nat. Neurosci.* **12**, 947-953.
Zheng, K., Wu, X., Kaestner, K. H. and Wang, P. J. (2009). The pluripotency factor LIN28 marks undifferentiated spermatogonia in mouse. *BMC Dev. Biol.* **9**, 38.
Zhu, H., Shyh-Chang, N., Segre, A. V., Shinoda, G., Shah, S. P., Einhorn, W. S., Takeuchi, A., Engreitz, J. M., Hagan, J. P., Kharas, M. G. et al. (2011). The Lin28/let-7 axis regulates glucose metabolism. *Cell* **147**, 81-94.